



Assessment of optimal growth conditions for biomass and exopolysaccharides production in the thermotolerant cyanobacterium *Phormidium* sp. ETS-05

Raffaella Margherita Zampieri¹ · Fabrizio Caldara² · Nicoletta La Rocca¹

Received: 15 March 2023 / Revised: 10 May 2023 / Accepted: 11 May 2023 / Published online: 29 May 2023
© The Author(s) 2023

Abstract

Phormidium sp. ETS-05 is one of the target cyanobacteria species conferring anti-inflammatory properties to the therapeutic muds applied by spas of the Euganean Thermal District (Italy) to treat arthro-rheumatic pathologies. Beneficial mud is prepared by spas following a traditional method, called maturation, leading to the growth of a specific microbiota on natural raw clay irrigated by flowing thermal water at 37–47 °C for about two months. The effectiveness of the mud is related to heat, electrolytes and bioactive molecules synthesized by the microbiota. A clear role in the anti-inflammatory activity of muds has been demonstrated for the exopolysaccharides, EPS, produced by the entire microbiota and *Phormidium* sp. ETS-05. Considering the interest in this species, we assessed its optimal growth conditions to obtain the higher EPS production in relation to temperature, light spectra, and intensity and nitrogen availability. The production of biomass and pigments was also taken into account, as other high-value compounds can be obtained in parallel with EPS. We found that exposure to a temperature of 45 °C under white light at 100 $\mu\text{mol photons m}^{-2} \text{s}^{-1}$ is optimal to reach the highest biomass (1.13 g L⁻¹) and an average production of 75 mg g_{DW}⁻¹ phycocyanin and of 150 mg g_{DW}⁻¹ EPS for *Phormidium* sp. ETS-05 cultured in lab-scale photobioreactors for 9 days. Putative genes linked with EPS assembly and export have also been identified in its genome, some of which have been investigated for their expression levels, opening up the possibility of biotechnologically boost EPS production.

Keywords *Phormidium* sp. ETS-05 · Thermal environment · Exopolysaccharides · Phycocyanin · Exopolysaccharides-related genes · Hormogonia

Introduction

Cyanobacteria are ubiquitous organisms, present in different ecosystems, including extreme environments, even characterized by temperatures up to 74 °C (Ward et al. 2012). To thrive in these habitats, they have developed great adaptability to varying conditions and several mechanisms to cope with different stressors (Kumar et al. 2018), leading to an extremely versatile metabolism. Cyanobacteria are indeed capable of synthesizing a wide range of primary and

secondary metabolites, making them a promising source of bioactive compounds, food and feed supplements, biopolymers, biofuels, biofertilizers, and can also be used for bioremediation, wastewater treatments, and CO₂ sequestering processes (Patel et al. 2019). Cyanobacteria are considered promising candidates for use in bioindustrial applications (Ducat et al. 2011) thanks to their low requirements needed for growth (sunlight, CO₂, water with few mineral nutrients) and the ability to increase the production of compound of interest by changing the growth parameters used.

Among hot environments, volcanic environments, hydrothermal vents, and hot springs are inhabited by thermotolerant, thermophilic, and hyper-thermophilic microorganisms (Patel et al. 2019). In hot springs, they commonly create microbial communities that form mats that are composed of primary producers, photoautotrophs (cyanobacteria, purple phototrophs, green phototrophs), and chemolithoautotrophs (Franks and Stolz 2009).

✉ Raffaella Margherita Zampieri
raffaellamargherita.zampieri@phd.unipd.it

¹ Department of Biology, University of Padua, Via Bassi 58/B, 35131 Padua, Italy

² Pietro d'Abano Thermal Studies Center, Via Jappelli 5, Abano Terme, 35031 Padova, Italy

The Euganean Thermal District (Padova, Italy) is an important thermal pole in Europe and is renowned for both thermal water treatments and pelotherapy (i.e. mud therapy). These are performed using natural resources of the territory: thermal water gushing at an average temperature of 75 °C and clay collected from local thermal lakes. The efficacy of mud therapies relies on thermal, mechanical, and biochemical factors (Fioravanti et al. 2011) that are inorganic and organic compounds accumulated by a specific microbiota that grows during the maturation of the mud starting from raw clay bathed with thermal water (Gris et al. 2020). The peculiarity of the Euganean mud lies in the growth of microorganisms during the maturation process, among which cyanobacteria play a leading role composing up to 30% of the total microbiota (Gris et al. 2020). Anti-inflammatory and antioxidant activity of polysaccharides extracted from the therapeutic mud was recently demonstrated by in vivo tests using zebrafish as model organism (Zampieri et al. 2022). Among cyanobacteria, *Phormidium* sp. ETS-05 (Ceschi Berrini et al. 2004) hereafter referred to as ETS-05, is the most abundant species (41% on average) up to 47 °C (Gris et al. 2020). This filamentous strain shows solitary trichomes that propagate due to the fragmentation by necridia and the development of hormogonia (Ceschi Berrini et al. 2004). The contribution of ETS-05 to the therapeutic activity of the Euganean mud has been investigated in vitro and in vivo, revealing that its exopolysaccharides (EPS), have anti-inflammatory activity (Zampieri et al. 2020).

EPS can be found in high concentrations in therapeutic muds, linked to the microbial cell surface or released into the environment, acting as a boundary between cells and their surroundings with several purposes: creation of biofilms, establishment of symbiosis, protection against desiccation and UV, and nutrients sequestration (Pereira et al. 2009). EPS are characterized by peculiar biological activities (anti-inflammatory, antiviral, antioxidant, antibacterial, immunostimulant) and physico-chemical properties (viscosity, water retention) that make them interesting for several fields: pharmaceutical, nutraceutical, cosmetic, food, and agriculture (Laroche 2022).

The mechanism responsible for EPS synthesis and release is relatively conserved throughout bacteria, even though limited information is available for cyanobacteria (Pereira et al. 2013). Three biosynthetic pathways have been described: Wzy-dependent, ABC transporter-dependent, and Synthase-dependent. For the first two pathways, two protein families are fundamental: polysaccharide copolymerase (PCP), that are respectively Wzc and KpsE, and outer membrane polysaccharide export (OPX), represented by Wza and KpsD proteins. OPX proteins possess conserved domains: a polysaccharide export sequence (PES or poly_export domain) and a soluble ligand-binding beta-grasp domain (SLBB) (Pereira et al. 2013). In Synthase-dependent pathway, polysaccharides are

simultaneously assembled and exported by synthase Alg8 or BcsA involved, respectively, in the production of alginate or cellulose (Pereira et al. 2015). In 2013 a polysaccharide secretion system was hypothesized to be linked to hormogonia formation and gliding motility in *Nostoc punctiforme* ATCC 29,133 (Risser and Meeks 2013; Khayatan et al. 2015). Hormogonia trichomes are functionally and morphologically diverse from vegetative filaments, being generally involved in dispersal events and shorter (Herdman and Rippka 1988). Hormogonium polysaccharides (HPS) synthesis gene set (*hps*) was identified; interestingly, a set of putative Hps proteins have been associated as members of the Wzy-dependent pathway (Zuniga et al. 2020a).

Different strategies can be applied to induce high EPS synthesis in different strains such as nutrient starvation (N, P, Mg²⁺, Ca²⁺) or stresses (high light, temperature, salinity). However, the best condition to increase EPS yield is rather species-specific as was nicely described by Pereira et al. (Pereira et al. 2009) and Laroche (Laroche 2022). Together with EPS, other high value compounds can be simultaneously produced, such as water- and lipid-soluble pigments. Phycobiliproteins and in particular phycocyanin (PC) have several bioactive properties: antioxidant, anticancer, anti-inflammatory, anti-diabetes, neuroprotective, and anti-obesity (Pagels et al. 2019).

In this study, ETS-05 was grown under different conditions. Temperatures (30, 35, 40, 45, 50 °C), light spectra (white, blue, green, yellow, red lights), light intensities (20, 50, 75, 100, 125, 150, 200, 400 μmol photons m⁻² s⁻¹) and nitrogen availability were tested to evaluate both biomass production and the synthesis of compounds of interest, focusing on EPS and PC. Optimal parameters resulted in 45 °C, 100 μmol photons m⁻² s⁻¹ of white light and with the presence of combined nitrogen source (NaNO₃) in the medium. The higher biomass obtained corresponded to 1.13 g L⁻¹ of biomass in 9 days of cultivation, together with an average of 150 mg g_{DW}⁻¹ of EPS and 75 mg g_{DW}⁻¹ of PC. In addition, genes linked to EPS synthesis have been found through a bioinformatic research in the ETS-05 genome. For some of these genes, *wza*, *wzc*, a gene coding for a protein involved in polysaccharide export (*ps_ex*) and a gene related to HPS synthesis (*hrmK*), the correlation between their expression level and the release of polysaccharides by ETS-05 was verified by Real-Time qPCR analysis.

Materials & methods

Cyanobacterium strain used and maintenance

Cultures of *Phormidium* sp. ETS-05 were available in the laboratory as a result of previous collaborations with the Pietro d'Abano Thermal Studies Center (Ceschi Berrini et al.

2004). Organism was maintained in flasks in a thermostatic chamber at 30 °C (± 1 °C) and 10 $\mu\text{mol photons m}^{-2} \text{s}^{-1}$ continuous white light. Medium for maintenance and growth of the cyanobacterium was BG11 (Rippka et al. 1979). For nitrogen starvation experiments, BG11₀ medium was used (Rippka et al. 1979), which lacks a nitrate source.

Experimental settings

Experiments culturing ETS-05 under diverse light spectra were conducted using cell culture flasks. The only source of light was given by stripes of LEDs covered in colored filters and spectra were assessed using LI-COR LI-180 spectrometer (Ecosearch Srl, Italy) (light spectra are presented in Fig. S1). For each light, 50 $\mu\text{mol photons m}^{-2} \text{s}^{-1}$ were obtained. The temperature was maintained constant at 30 °C. ETS-05 was exposed to the lights for 9 days starting from inocula cultivated for 10 days in white light and diluted to the starting concentration of 0.2 g (dry weight) L⁻¹. Experiments were conducted with 4 biological replicates.

For the subsequent tests, the organism was cultivated using the Photobioreactor Multi-cultivator MC-1000 OD system (Photon Systems Instruments, Czech Republic). ETS-05 was pre-adapted to the photobioreactor system. Cultures were grown for 10 days starting from and optical density (OD) at 750 nm of 0.4 at 30 °C and 50 $\mu\text{mol photons m}^{-2} \text{s}^{-1}$ of constant light. The LED spectrum (cold white light) is available in Multi-cultivator MC-1000 OD manual (www.psi.cz). A constant flux of filtered atmospheric air bubbles kept the filament in suspension in the medium. Cells were firstly centrifuged to eliminate residues of released compounds present in the medium that could have altered measurements or growth. Inocula were obtained by resuspending the cultures to an OD_{750nm} of 0.2 with a final volume of 80 mL for each tube. The growth curves for testing different temperatures were performed at 50 $\mu\text{mol photons m}^{-2} \text{s}^{-1}$, while the light intensities curves were completed at 45 °C. Six biological replicates were performed for each condition tested.

For tests related to nitrogen starvation, 45 °C and 100 $\mu\text{mol photons m}^{-2} \text{s}^{-1}$ were used. A two-step cultivation was performed to stimulate the growth of the organism. After 9 days of growth in BG11, cells were centrifuged and resuspended in BG11 or BG11₀. Experiments lasted an additional 9 days and were conducted with 4 biological replicates.

Growth and biomass quantification

Growth was assessed for 9 days. OD_{750nm} was measured using a spectrophotometer, sampling at 0, 2, 4, 7 and 9 days. Biomass was also assessed as dry weight of 5 mL of culture using 0.45 μm filters. Dry weight was measured at the

starting and end point (day 9) of the experiments. For OD measures, two samplings were made for each culture and 5 measurements were performed for each sample. The consistency between OD_{750nm} data and dry weight measurements was also assessed.

In vivo absorption spectra

To assess light absorption features of ETS-05, in vivo spectra were measured. Cells were centrifuged at 3000 $\times g$ for 5 min and pellets were carefully homogenized to disaggregate cells. After resuspending, samples were analyzed at a spectrophotometer using quartz cuvettes. According to literature (Gan et al. 2014), the opaque sides of the cuvettes were crossed by the ray, to correct for scattering.

Chlorophyll a, carotenoids and phycobiliproteins extraction and quantification

For the extraction of lipophilic pigments, organism was sampled at 0, 2, 4, 7 and 9 days after growth and centrifuged at 20,000 $\times g$. Pellet was then resuspended in N, N-dimethylformamide (Sigma-Aldrich, USA) and incubated at 4 °C for 24 h in the dark. Supernatant obtained from centrifugation was then analyzed spectrophotometrically using the absorption spectrum from 350 to 750 nm. Chlorophyll *a* and carotenoids concentrations were calculated according to equations from (Moran 1982) for chlorophyll *a* and (Chamovitz et al. 1993) for carotenoids:

$$\begin{aligned} \text{Chlorophyll } a \text{ (}\mu\text{g mL}^{-1}\text{)} &= A_{664} \times 11.92 \\ \text{Carotenoids (}\mu\text{g mL}^{-1}\text{)} &= A_{461} - (0.046 \times A_{664}) \times 4 \end{aligned}$$

where A_{461} and A_{664} are the absorbance values at 461 and 664 nm, respectively.

For the extraction of hydrophilic pigments, samples collected at the beginning and at the end (9 days) of the growth curves were centrifuged at 20,000 $\times g$ to remove residual traces of medium. An equal volume of glass beads (150–212 μm) was then added to the pellet with cold phosphate buffer (NaCl 0.15 M, Na₂HPO₄ 0.01 M, pH 9). Cells were disrupted with three cycles of bead beater (3500 OPM, 30 s) alternated with 30 s in ice. Supernatant obtained after centrifugation (20,000 $\times g$, 4 °C) was collected in a clean tube and the pellet was resuspended in cold phosphate buffer. This step was repeated until a transparent supernatant was obtained. The accumulated supernatant was centrifuged again to eliminate eventual remaining cells or membranes. The whole spectrum was measured at the spectrophotometer from 350 to 750 nm. As reported in (Bennett and Bogorad 1973) for phycocyanin (PC) and allophycocyanin (APC) and in (Kaplan et al. 1986) for phycoerythrocyanin (PEC):

$$\text{Phycocyanin (mg mL}^{-1}\text{)} = [A_{615} - (0.474 \times A_{652})]/5.34$$

$$\text{Allophycocyanin (mg mL}^{-1}\text{)} = [A_{652} - (0.208 \times A_{615})]/5.09$$

$$\text{Phycocerythrocyanin (mg mL}^{-1}\text{)} = A_{572} - (0.619 \times A_{612}) + (0.088 \times A_{647})/5.775$$

where A_{572} , A_{612} , A_{615} , A_{647} and A_{652} correspond to absorbance values at 572, 612, 615, 647, and 652 nm. Values of chlorophyll *a*, carotenoids, and phycobiliproteins concentrations were then referred to the biomass expressed as dry weight.

Exopolysaccharides' extraction and quantification

EPS were collected at the beginning of the experiment and after 9 days, corresponding to the final point. Method followed is described in (Gris et al. 2017). Quantification was performed using sample, 5% phenol and sulfuric acid in the ratio 1:1:5 according to the Dubois method (DuBois et al. 1956). Optical density at 488 nm was measured and the EPS concentration was referred to a glucose calibration curve. EPS concentration was correlated to the biomass of the cultures expressed as dry weight.

Optical microscopy and Transmission Electron Microscopy (TEM) analyses

ETS-05 exposed to different light intensities was observed through light microscopy (Axiophot, Zeiss, equipped with a Leica EC3 camera), and images were acquired moving on the diagonals of the slides. 10X magnification was used to clearly see the filaments in their whole extension. For each condition, 100 filaments were measured in their length using the software ImageJ (Schneider et al. 2012).

TEM images were acquired for samples at the starting point and cultivated for 9 days at 45 °C under 25 or 100 $\mu\text{mol photons m}^{-2} \text{s}^{-1}$ of white light. According to La Rocca et al. (La Rocca et al. 2015), cells were centrifuged (10 min, 17,000 $\times g$) and fixed overnight at 4 °C in 3% glutaraldehyde in 0.1 M sodium cacodylate buffer (pH 6.9) and post-fixed for 2 h in 1% osmium tetroxide in the same buffer. The samples were dehydrated in a graded series of ethyl alcohol and propylene oxide and embedded in Araldite. Ultrathin sections (80–100 nm) were cut with an ultramicrotome (Ultracut; Reichert-Jung, Austria) and stained with lead citrate and uranyl acetate. Analysis was conducted under a transmission electron microscope (Tecnai G2; FEI, USA) operating at 100 kV.

Real-Time qPCR analysis and research of genes of interest

ETS-05 genome was previously submitted as BioProject PRJNA622676 (Gris et al. 2020), available in NCBI (NIH). Nucleotide BLAST and tBLASTn (NIH) were used to search for genes of interest. Query sequences were selected from

the strains phylogenetically closer to ETS-05 based on previous analyses (Pereira et al. 2013, 2015). Other candidate sequences were searched in genome annotation using keywords “polysaccharides”, “exopolysaccharides”, and “export”. Operon-mapper (Taboada et al. 2018) was used to implement or confirm the annotation described in Gris et al. 2020. Pfam (Mistry et al. 2021) and InterPro (Paysan-Lafosse et al. 2022) were used to identify protein families.

Samples collected at the beginning of the experiment and after 2 days were centrifuged at 10,000 $\times g$ and pellets were stored at -20 °C. Glass beads (acid-washed, 150–212 μm , Sigma-Aldrich) and 1 mL of TRI Reagent (Sigma-Aldrich) were added to the frozen pellets and cells were disrupted with 3 cycles of bead beater (10 s, 3000 OPM) alternated with storage on ice for 30 s. Samples were kept for 10 min at room temperature after adding 0.2 mL of chloroform. Centrifugation of the samples at 12,000 $\times g$ for 15 min at 4 °C allowed collection of the upper phases containing RNA. These were moved to a clean tube with 0.5 mL of isopropanol and incubated for 10 min at room temperature. After centrifugation pellets were washed with 1 mL of 75% ethanol. A subsequent centrifugation step allowed the ethanol to be discarded and the pellets were resuspended in DEPC-treated water. RNA was concentrated and purified using RNA Clean and Concentrator (Zymo Research, USA), after incubation of samples for 15 min at room temperature with DNase I and DNA Digestion Buffer (Zymo Research). The absence of genomic DNA was verified by PCR using ThermoScientific DreamTaq Green PCR Master Mix (2 \times , Thermo Fisher Scientific, USA) and *gyrB* primers, following the manufacturer's instructions. The resulting reactions were then run on agarose gel electrophoresis. cDNA was obtained using RevertAid Reverse Transcriptase (Thermo Fisher Scientific) according to the manufacturer's instructions. Real-Time qPCRs were performed in a CFX384 Touch Real-Time PCR Detection System (Bio-Rad Laboratories, USA). Primer sequences are reported in Table S1. Data were normalized to the expression of *gyrB* to standardize the results by eliminating variation in cDNA quantity and quality (Cusick et al. 2015). The cycling parameters were 95 °C for 10 min, followed by 45 cycles at 95 °C, annealing (60 °C) and extension for 30 s. No amplification products were observed in negative controls, and no primer-dimer formations were observed in the control templates. qPCR results were analyzed using the $\Delta\Delta\text{Ct}$ method using the Bio-Rad CFX Manager software version 3.1 (Bio-Rad Laboratories). Three biological replicas of the experiments were performed with technical triplicates for each reaction.

Statistical analysis

Statistical analyses were performed using GraphPad Prism (9.4.1, GraphPad Software, USA). One-way ANOVA with

Tukey's multiple comparison test was used for all experiments. An exception was made for the nitrogen starvation test, in which only two groups of data were considered, therefore Two-tailed Unpaired t test was applied. P values are reported in figures or tables.

Results

Growth of ETS-05 under different light spectra

Preliminary analysis was conducted by exposing the organism to different light spectra, enriched in the wavelengths of blue, green, yellow, and red and compared to white light spectra. After 9 days of growth, higher biomass production, reported as dry weight, was achieved under white, yellow, and red light (Fig. 1a). Slightly lower values were observed in green light and drastic altered growth in blue light, reaching a mean dry weight of only 0.25 g L^{-1} . No appreciable difference could be seen in the in vivo absorption spectra (Fig. S2), suggesting that the organism did not activate any kind of chromatic acclimation (Hirose et al. 2019; Sanfilippo et al. 2019). Considering chlorophyll *a*, carotenoids, and phycobiliproteins content (Table 1) lower amounts were obtained when cells were exposed to blue light, while no substantial differences were observed for the other lights. Similar results were obtained also for EPS production (Fig. 1b), with blue light being less

interesting for production of these compounds. Excluding blue lights in which not only growth but also production of pigments and EPS were lower, no statistically significant differences were observed between other conditions for the mentioned parameters. Following experiments were therefore conducted using white light.

Assessment of the temperature optimum for growth and production of biomolecules

Temperatures from 30 to 50 °C were tested. Biomass growth reported as $\text{Log OD}_{750\text{nm}}$ (Fig. 2a) and dry weight (Table 2), did not change between 30, 40 and 45 °C. A drastic impairment in growth was observed for the higher temperature tested, 50 °C, causing the death of the organisms after 4 days. EPS (Fig. 2b) obtained from the supernatant at the end of the growth curves were quantified and were directly correlated with the temperature. Higher value of $48 \text{ mg g}_{\text{DW}}^{-1}$ was reached at 45 °C. Phycocyanin, the most abundant pigment produced by ETS-05, was quantified at the end of the experiments. Its concentration increased up to 40 °C ($222 \text{ mg g}_{\text{DW}}^{-1}$), while it lowered by half at 45 °C ($115 \text{ mg g}_{\text{DW}}^{-1}$). 50 °C condition was not evaluated at 9 days since no viable cell was present in culture, as can be appreciated by the whitish color of tube 50 in Fig. 2a.

Phycobiliprotein content increased with the temperature, in parallel with the concentrations of chlorophylls and

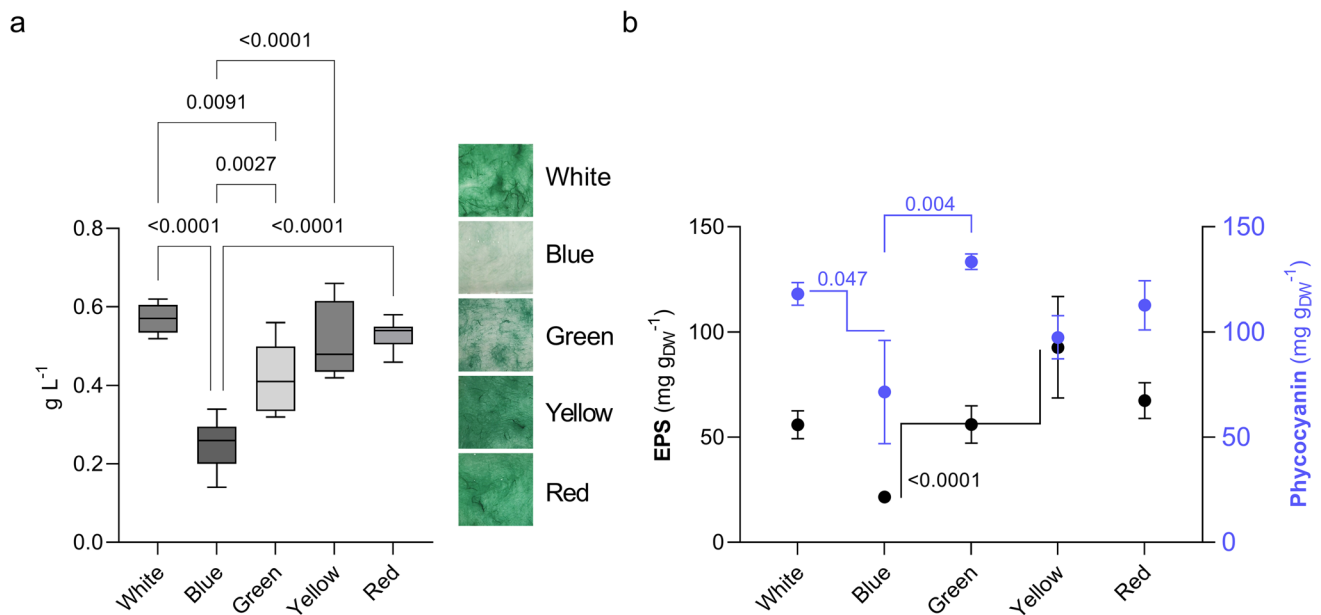


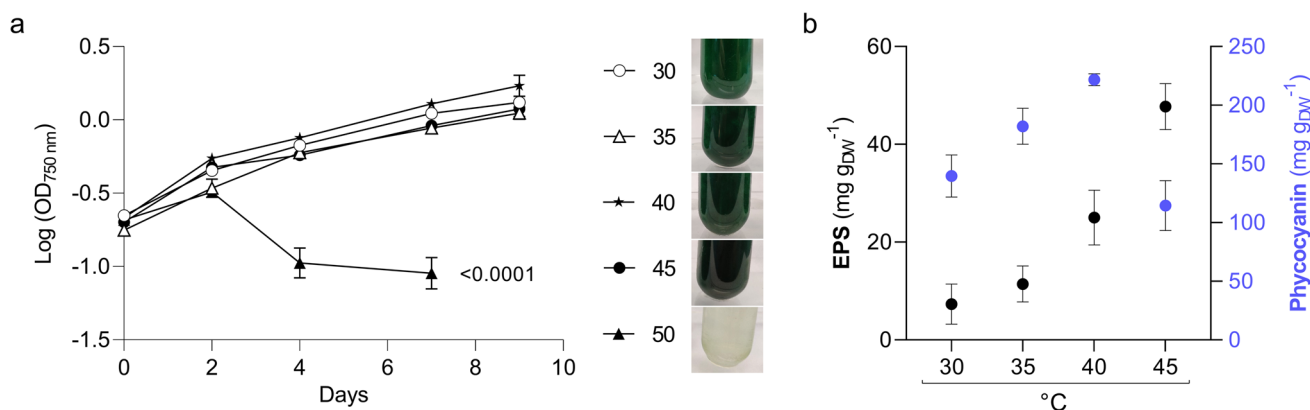
Fig. 1 Growth of *Phormidium* sp. ETS-05 exposed to different light spectra: white, blue, green, yellow, and red. (a) Biomass after 9 days of growth reported as g L^{-1} . Images of the cultures in the flasks at the end of the experiment. Mean is indicated by the horizontal line,

min and max values are shown by the bars. (b) Production of EPS (black) and phycocyanin (blue) after 9 days of growth, related to the dry weight of the cultures. Bars indicate mean with standard deviation. P values are reported ($n=4$)

Table 1 Quantification of biomass as dry weight and of extracted pigments after 9 days of growth of *Phormidium* sp. ETS-05 exposed to different light spectra.^a

	Biomass (g L ⁻¹)	APC (mg g _{DW} ⁻¹)	PC	PEC	Chl <i>a</i>	Car	Chl <i>a</i> /Car
White	0.57 ± 0.04	51.8 ± 3.5	118.6 ± 5.3	13.0 ± 2.7	15.1 ± 3.9	2.4 ± 0.6	6.1
Blue	0.25 ± 0.07	19.7 ± 9.5	71.5 ± 24.6	4.9 ± 2.3	12.5 ± 5.4	1.7 ± 0.7	7.3
Green	0.42 ± 0.1	34.1 ± 9.3	133.4 ± 3.7	9.7 ± 1.9	14.0 ± 2.7	2.2 ± 0.6	7.0
Yellow	0.51 ± 0.1	39.3 ± 3.3	97.5 ± 10.2	8.8 ± 3.3	14.1 ± 1.3	2.3 ± 0.2	6.2
Red	0.53 ± 0.04	42.3 ± 12.6	112.7 ± 11.6	10.9 ± 4.7	13.1 ± 3.7	1.9 ± 0.6	6.8

^a Concentrations are referred to the dry weight. Higher values are indicated in bold. Means ± standard deviations are reported. *APC* allophycocyanin, *PC* phycocyanin, *PEC* phycoerythrocyanin, *Chl a* chlorophyll *a*, *Car* carotenoids

**Fig. 2** Growth of *Phormidium* sp. ETS-05 at increasing temperatures from 30 to 50 °C. (a) Growth curves reported as Log (OD_{750nm}); legend also depicts cultures in tubes after 9 days. (b) Production of EPS

(black) and phycocyanin (blue) after 9 days of growth, related to the dry weight of the cultures. Bars indicate mean with standard deviation (n=6). P values are reported for (a), and are in Table S2 for (b)

carotenoids (Table 2). Lipid-soluble pigment concentrations increased in time in a similar way among the conditions evaluated (Fig. S3), and no difference was assessed in the Chl *a*/Car ratio, indicating that these pigments composition is not influenced by the temperatures tested.

ETS-05 can be ascribed to mesophilic or lower thermophilic bacteria having the optimal temperature for growth between 40 and 45 °C.

Analysis of growth under different light intensities and nutrients

Considering previous results obtained, further experiments were conducted at 45 °C, with the aim of gaining the higher biomass together with the higher amount of EPS in the supernatant. Increasing light intensities were tested from 25 to 400 μmol photons m⁻² s⁻¹. Lowest and highest light tested

Table 2 Quantification of biomass as dry weight and of extracted pigments after 9 days of growth of *Phormidium* sp. ETS-05 at the tested temperatures.^a

°C	Biomass (g L ⁻¹)	APC (mg g _{DW} ⁻¹)	PC	PEC	Chl <i>a</i>	Car	Chl <i>a</i> /Car
30	0.93 ± 0.01	48.2 ± 9.1	139.7 ± 16.2	3.8 ± 1.1	12.9 ± 1.1	2.4 ± 0.1	5.7
35	0.92 ± 0.02	56.0 ± 4.5	182.1 ± 13.2	17.1 ± 3.3	15.4 ± 1.4	3.1 ± 0.3	5.4
40	0.94 ± 0.01	52.9 ± 3.7	221.8 ± 9.9	22.5 ± 4.8	22.9 ± 2.3	4.3 ± 0.4	5.3
45	0.95 ± 0.07	38.1 ± 9.2	114.5 ± 18.9	21.2 ± 4.9	19.9 ± 2.6	3.7 ± 0.7	5.4

^a Concentrations are referred to the dry weight. Higher values are indicated in bold. Means ± standard deviations are reported. *APC* allophycocyanin, *PC* phycocyanin, *PEC* phycoerythrocyanin, *Chl a* chlorophyll *a*, *Car* carotenoids

both determined a reduction in the growth of the cultures (Fig. 3a). No statistical difference was detected between 50, 75, 100, 125, 150 and 200 $\mu\text{mol photons m}^{-2} \text{s}^{-1}$ for both $\text{OD}_{750\text{nm}}$ and biomass measured as dry weight (Table 3), with 100 $\mu\text{mol photons m}^{-2} \text{s}^{-1}$ reaching higher values. EPS production (Fig. 3b) increased in parallel with the increasing light, with lights 75 and 100 reaching 3 times (143.4 ± 58.3 and $140.4 \pm 39.9 \text{ mg g}_{\text{DW}}^{-1}$, respectively) the EPS produced at 25 and 50 $\mu\text{mol photons m}^{-2} \text{s}^{-1}$ (respectively 50.7 ± 39.1 and $60.5 \pm 36.2 \text{ mg g}_{\text{DW}}^{-1}$) while a fivefold increase was measured for 125, 150 and 200 $\mu\text{mol photons m}^{-2} \text{s}^{-1}$ (in order: 241.9 ± 85.4 , 263.8 ± 72.1 , $218.6 \pm 56.8 \text{ mg g}_{\text{DW}}^{-1}$). The values reached at 400 $\mu\text{mol photons m}^{-2} \text{s}^{-1}$ ($434.3 \pm 98.9 \text{ mg g}_{\text{DW}}^{-1}$) could have been misrepresented by the presence of cellular polysaccharides released by dead cells. The presence of this substantial quantity of EPS could otherwise represent a response to the stress condition caused by high light. Phycocyanin quantification showed the opposite trend, with augmented production at lower light

intensities. Indeed, at 25 $\mu\text{mol photons m}^{-2} \text{s}^{-1}$ a higher quantity corresponding to $116 \text{ mg g}_{\text{DW}}^{-1}$ was observed, drastically reducing to only $14 \text{ mg g}_{\text{DW}}^{-1}$ at 25 $\mu\text{mol photons m}^{-2} \text{s}^{-1}$. The difference in pigment content is reflected in the coloration of the cultures from a macroscopic point of view.

Considering all the quantified pigments (Table 3), phycobiliproteins showed the highest variability according to the condition tested. Allophycocyanin aside, which decreased 2 or 4 times from 25 to 400 $\mu\text{mol photons m}^{-2} \text{s}^{-1}$, phycocyanin and phycoerythrocyanin were the most variable, with a tenfold change, implying the leading role of these molecules in the response to the lights given. Chlorophyll *a* and carotenoids contents were more stable across the intensities tested, decreasing mainly at 200 and 400 $\mu\text{mol photons m}^{-2} \text{s}^{-1}$. These pigments quantity increased for each light intensity tested for the duration of the experiments in a similar way (Fig. S4), correlating with the increase in time of the optical density. The ratio between these two classes of pigments was lower

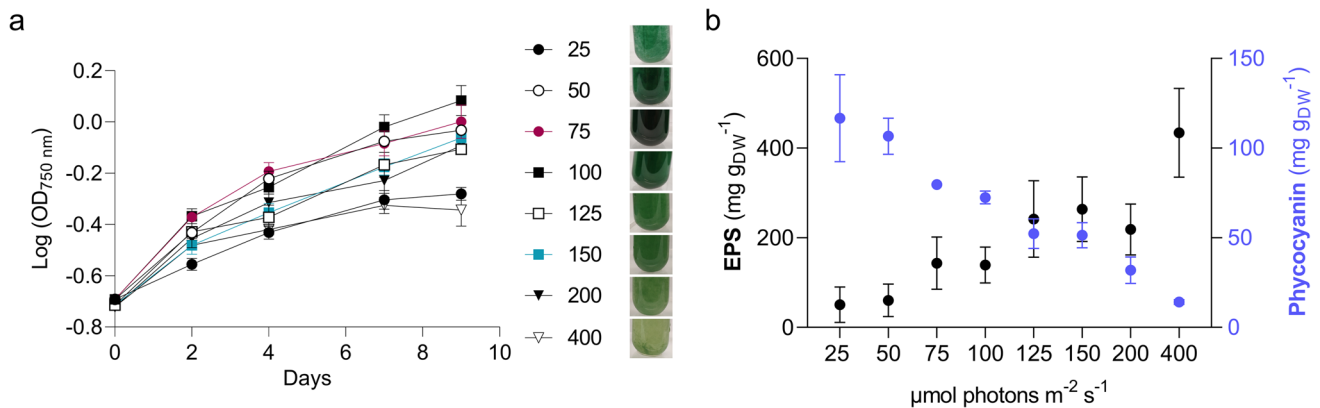


Fig. 3 Growth of *Phormidium* sp. ETS-05 at different light intensities, from 25 to 400 $\mu\text{mol photons m}^{-2} \text{s}^{-1}$. (a) Growth curves reported as $\text{Log}(\text{OD}_{750\text{nm}})$; legend also depicts cultures in tubes after 9 days. (b) Production of EPS (black) and phycocyanin (blue) after

9 days of growth, correlated to the dry weight of the cultures. Bars indicate mean with standard deviation ($n=6$). Statistical analysis with comparisons tests is reported in Tables S3, S4 and S5

Table 3 Biomass of *Phormidium* sp. ETS-05 produced and pigment content after 9 days of growth under different light intensities (from 25 to 400 $\mu\text{mol photons m}^{-2} \text{s}^{-1}$).^a

	Biomass (g L^{-1})	APC ($\text{mg g}_{\text{DW}}^{-1}$)	PC	PEC	Chl <i>a</i>	Car	Chl <i>a</i> /Car
25	0.39 ± 0.16	32.1 ± 3.1	116.7 ± 14.3	12.4 ± 2.1	9.6 ± 0.1	2.3 ± 0.5	4.3
50	0.76 ± 0.14	33.6 ± 1.9	106.7 ± 10.1	20.7 ± 4.1	11.9 ± 1.2	2.8 ± 0.4	4.8
75	0.89 ± 0.38	25.5 ± 2.4	79.7 ± 2.6	15.7 ± 2.8	10.9 ± 0.8	2.1 ± 0.3	5.7
100	1.13 ± 0.32	26.7 ± 3.2	72.5 ± 3.5	16.7 ± 2.6	10.6 ± 0.5	2.2 ± 0.4	5.3
125	0.63 ± 0.10	15.1 ± 2.3	52.3 ± 8.2	3.6 ± 1.3	9.3 ± 0.8	2.1 ± 0.5	4.9
150	0.71 ± 0.10	16.9 ± 2.4	51.3 ± 6.9	3.2 ± 0.2	9.7 ± 1.0	2.1 ± 0.2	4.6
200	0.75 ± 0.06	12.3 ± 3.7	31.9 ± 7.4	2.4 ± 0.5	7.9 ± 2.5	1.8 ± 0.4	4.3
400	0.55 ± 0.11	7.3 ± 1.2	14.2 ± 1.2	0.7 ± 0.1	4.6 ± 0.6	1.6 ± 0.5	3.1

^a Concentrations of pigments are referred to the dry weight. Higher values are highlighted in bold. Means \pm standard deviations are reported. APC allophycocyanin, PC phycocyanin, PEC phycoerythrocyanin, Chl *a* chlorophyll *a*, Car carotenoids

at the extreme light intensities tested (25 and 400 $\mu\text{mol photons m}^{-2} \text{s}^{-1}$) mostly due to the smaller quantity of chlorophylls.

100 $\mu\text{mol photons m}^{-2} \text{s}^{-1}$ was established as optimal for ETS-05, reaching higher biomass and both an average phycocyanin and EPS production.

Having determined growth optima for both temperature and light intensity, different medium composition were tested to boost EPS release. Salt exposure led to cell death after 2–4 days even at the lowest concentration tested of 0.01 M, indicating that the stress caused was too detrimental for ETS-05 (data not shown).

To assess the effect of nitrogen on EPS production, knowing that ETS-05 is not able to fix atmospheric nitrogen (Ceschi Berrini et al. 2004), BG11₀ was used. After a preliminary experiment performed using optima parameters found, testing in parallel medium with or without NaNO_3 , the absence of the nutrient was verified to prevent its growth. A two-step growth was then examined (Fig. S5), using as starting point biomass grown for 9 days in ideal conditions, and refreshed then in the two different media. After 4 days of comparable growth, absence of NaNO_3 caused a decline in biomass. This led to a reduction in both EPS and PC synthesis. Similar results were obtained for all quantified pigments (Table S6). Therefore, cultivation of ETS-05 in absence of a nitrogen source was not improved, considering biomass and, more importantly, EPS production.

Light intensity affects filament length and hormogonia formation

To further characterize the response of the ETS-05 to the different light intensities, cultures were observed under light microscopy. Cells were observed after 4 days of growth, in

the exponential phase. A difference in the aspect of the cultures was observed, with the presence of shorter filaments in lights higher than 100 $\mu\text{mol photons m}^{-2} \text{s}^{-1}$. Trichomes were measured in their length (Fig. S6). At lower light intensities (Fig. 4a), filaments were longer with a mean length of 770 μm at 25 $\mu\text{mol photons m}^{-2} \text{s}^{-1}$ and 580 μm at 50 and 75 $\mu\text{mol photons m}^{-2} \text{s}^{-1}$. ETS-05 in these cases reached even a length of more than 1500 μm . At light intensities higher than 100 $\mu\text{mol photons m}^{-2} \text{s}^{-1}$ mean length resulted in 160 μm , with filaments as short as 10–20 μm (corresponding to 5–10 cells per filament).

For all intensities analyzed, 40–50% of the trichomes were 100–500 μm long (Fig. 4b). The main difference was visible in the lower and higher range of size considered: for lower light intensities (25, 50 and 75 $\mu\text{mol photons m}^{-2} \text{s}^{-1}$), 40–50% of the filaments were longer than 500 μm , while for light intensities higher than 100 $\mu\text{mol photons m}^{-2} \text{s}^{-1}$, 40–50% of them measured less than 100 μm in length. These short filaments could be hormogonia, transient cell forms differentiated from vegetative trichomes hypothesized to be involved in EPS release.

Going deeper in detail of the morphology, the sample grown in low light (25 $\mu\text{mol photons m}^{-2} \text{s}^{-1}$) and the optimal light intensity found (100 $\mu\text{mol photons m}^{-2} \text{s}^{-1}$) were investigated by electron microscopy (Fig. S7). The dimension and shape of the cells did not change between the two conditions (Fig. S7). No differences were detected in the internal organization: cells are packed with thylakoids that occupy most of the volume, arranged in fascicles. Nothing distinctive was observed comparing ETS-05 at the beginning, and after 9 days of growth.

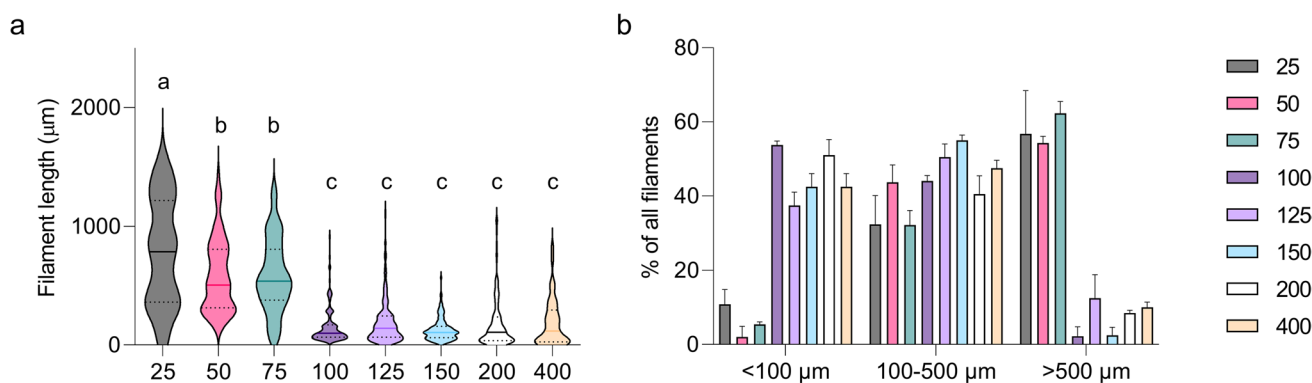


Fig. 4 Length of *Phormidium* sp. ETS-05 trichomes measured after 4 days of growth at different light intensities ($n=3$). **(a)** Distribution of the measured filaments from 0 to 2000 μm for the light intensities tested. Bold lines represent median, while dotted lines indicate

quartiles. Tukey's multiple comparisons test: a vs. b $p<0.01$, a vs. c $p<0.0001$, b vs. c $p<0.0001$ **(b)** Percentage of filaments per light intensity in three ranges: <100 μm , 100–500 μm and >500 μm . Bars indicate mean with standard deviation

Identification of genes linked to EPS assembly and export in ETS-05 genome

Proteins from other cyanobacterial species (Table S7) putatively related to the Wzy-dependent and ABC-dependent pathways were aligned with ETS-05 translated genome using tBLASTn (Table S8). Genes coding for PCP and OPX proteins are numerous and different within the same organism, leading to variability in the percentages of identity and query cover. Identities with OPX proteins (*Wza*/*KpsD*) had an average of 46%, while for PCP proteins (*Wzc*/*KpsE*) this value lowered to 42%. Considering the Wzy-dependent pathway, higher identities were reached by *Wzb*, that together with *Wzy*, are ubiquitously present in cyanobacteria according to (Pereira et al. 2015). Low percentages of identity and query cover were found for *Wzx* that is less conserved. As for ABC-dependent pathway, high levels of identity were observed for *KpsM* and *KpsF* (average 52%) while *KpsC*/*KpsS*, *KpsT*, *KpsU* had both minimal identity and query cover values, as expected from the low conservation of protein among cyanobacteria. No similarity was found for proteins involved in the Synthase-dependent pathway, using *Synechocystis* Alg8/*BscA* and other bacterial *BscC* sequences as query in tBLASTn. Other considered pathways were associated with polysaccharide release by hormogonia, or HPS (Tables S9 and S10, sequences are reported in Supplementary File 2). High percentages of identity were observed for all the genes investigated (average of 69%), with no significant similarity found only for genes *pilA*, *pilB*, *hpsB*, *hpsC*, *hpsG*, *hpsH* and *hpsM*. Interestingly, the gene clusters found in *N. punctiforme* are also maintained in ETS-05.

Finally, analyzing the annotated genes, other candidates were identified as possibly involved in EPS production (Table S11, sequences are reported in Supplementary File 2). In particular, AHNDPDGK_00533 gene codes for a “periplasmic protein involved in polysaccharide export” and contains a poly-export domain, typical of OPX proteins. Protein coded by gene AHNDPDGK_01089 is annotated by Operon-mapper as “putative polysaccharide export protein *wza*”, presents a poly-export domain and 4 SLBB domains, typical of OPX protein family. Similar results were obtained for AHNDPDGK_03356, annotated as “protein involved in polysaccharide export” and shortened as *ps_ex*, with a poly-export domain and 5 SLBB domains.

Transcription analysis of genes linked with EPS production and hormogonia formation

The involvement of low light and optimal light intensities in EPS release was investigated through gene expression analysis. Genes identified in ETS-05 genome and further

analyzed were *wzc* and *wza*, both part of the Wzy-dependent pathway, responsible for the assembly and release of EPS (Pereira et al. 2013) and HPS (Zuniga et al. 2020a). Gene *ps_ex* was identified in the genome annotation, as mentioned. Finally, *hrmK* was described in (Zuniga et al. 2020b) as fundamental for hormogonia formation and therefore associated with HPS production. For all genes (Fig. 5), the increase in expression was assessed after 2 days of growth in both 25 and 100 $\mu\text{mol photons m}^{-2} \text{s}^{-1}$. While no difference between low and optimal light was measured for *wza*, a twofold increase was observed for *wzc* at optimal light. This result suggests that the protein involved in the assembly of the EPS could play a fundamental role in their production, determining the boost in EPS quantity assessed in higher light intensities, rather than the protein implicated in the release itself. A significant rise in the expression of *ps_ex* was measured at 100 $\mu\text{mol photons m}^{-2} \text{s}^{-1}$ compared to the initial time point, but not at 25 $\mu\text{mol photons m}^{-2} \text{s}^{-1}$. A similar result was obtained for *hrmK* expression, giving another hint of involvement in hormogonia formation under high light intensities, and possibly the augmented polysaccharide production due to HPS release.

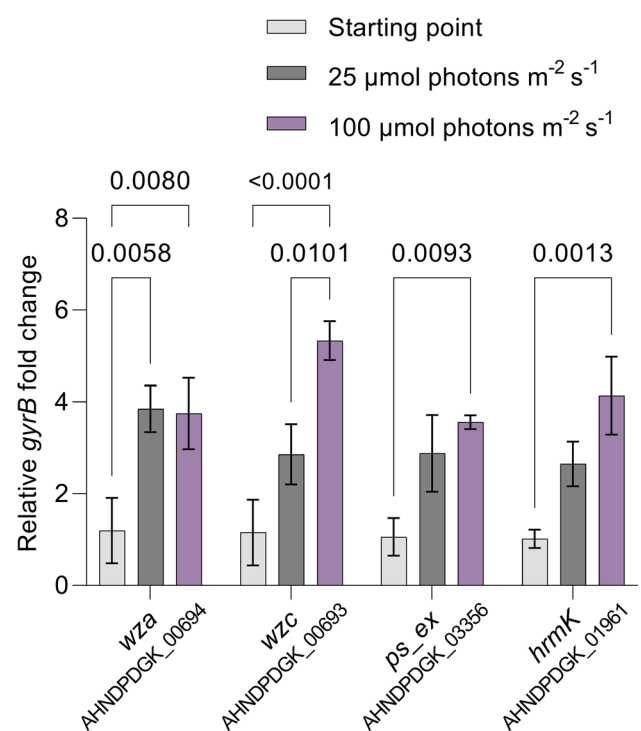


Fig. 5 Real-Time qPCR analysis of genes of *Phormidium* sp. ETS-05 linked with EPS production and release at two different light intensities: 25 and 100 $\mu\text{mol photons m}^{-2} \text{s}^{-1}$, compared to reference gene *gyrB*. Bars indicate mean with standard deviation. P values are reported. (n = 3)

Bioinformatic analysis of genes responsible for cyanotoxins synthesis

As thoroughly indicated, ETS-05 have been reported to produce diverse compounds of interest. Nonetheless, considering the relevance of the species in the production of the Euganean therapeutic mud, the potential production of cyanotoxins was considered. Genes responsible for the synthesis of most known cyanotoxins were searched in ETS-05 genome (Table S12). Microcystin and cylindrospermopsin (hepatotoxic), saxitoxin (neurotoxic) and lyngbyatoxin (dermatotoxic) (Merel et al. 2013) were not found, suggesting the inability of the strain to produce and release these compounds.

Discussion

The importance of ETS-05 in the context of therapeutic muds of the Euganean District led to the interest in analyzing the growth optima of this strain. ETS-05 represents, in fact, a source of high value compounds and could be exploited to both enrich the presence of the strain in the mud microbiota and to optimize its cultivation for biotechnological purposes. Considering the interest in EPS released by ETS-05, temperature, light spectra, light intensity, and nitrogen availability were evaluated not only to observe the culture response, but also to boost their production. Since EPS are obtained from the supernatant, intracellular high value compound production could be linked to the EPS one. Phycocyanin for instance was considered for its use in several fields (pharmaceutical, food, cosmetic (Saini et al. 2018)).

Effect of light spectra on growth was considered, since red and yellow lights (de Mooij et al. 2016; Toyoshima et al. 2020) are generally more effective. Moreover Baer et al. (Baer et al. 2016) showed the importance of determining the optimized RGB mixture for each species. ETS-05 growth was not drastically influenced by light spectra, other than blue light, that determined a drastic reduction in the biomass compared to other lights tested, as described in *Synechococcus elongatus* with 50 $\mu\text{mol photons m}^{-2} \text{s}^{-1}$ (Ooms et al. 2017) and for *Arthrospira platensis* comparing red and blue light (Lima et al. 2018). According to Han and colleagues (Han et al. 2015), both red and blue monochromatic lights enhanced EPS production in *Nostoc flagelliforme*, compared to white light exposure. However, in our study, ETS-05 did not show improvements in EPS release using other lights rather than white light. Similar results were obtained for *Nostoc calcicola* RDU-3 with higher growth and polysaccharides release under white light followed by yellow, red, green, and blue lights (Singh and Das 2011). Some cyanobacteria can perform photoacclimation processes called chromatic acclimations (CA), involving the regulation of

photosystems I and II and of phycobilisomes (Sanfilippo et al. 2019). Bioinformatic analysis data suggest that some *Phormidium* strains may perform CA7, a modulation in the quantity of PEC according to the light spectrum (Hirose et al. 2019). Chromatic acclimation in red and green light was described in *Phormidium* sp. C86, with more synthesis of PE in green light and of PC in red light (Westermann and Wehrmeyer 1995). Alteration in PE and PC content was also observed in *Phormidium autumnale* CCAP1462/10 (Palinska et al. 2011). No change in pigmentation was observed in ETS-05, other than a diminished amount of all pigments in blue light, therefore, the strain seems not able to perform any known kind of chromatic acclimation.

Thermotolerance of the species, anticipated considering its presence during the mud maturation process up to 47 °C (Gris et al. 2020), determined that higher biomass should be reached at 45 °C. Higher temperature tested of 50 °C led nonetheless to the death of the organisms at 4 days, after a slight increase in $\text{OD}_{750\text{nm}}$ in the first days of cultivation. At the optimal temperature for biomass, higher EPS production was also obtained, as tested in cyanobacteria *Scytonema tolypothrichoides* and *Tolypothrix bouteillei* (Kvíderová et al. 2019). There was a direct correlation between temperature and EPS release. Same correlation was observed for PC up to 40 °C where larger quantities were obtained: $221.8 \pm 9.9 \text{ mg g}_{\text{DW}}^{-1}$. The content of PC in this condition was up to 21% $\text{w w}_{\text{DW}}^{-1}$, similar to *A. platensis* (Xie et al. 2015), the most productive source of PC (Nwoba et al. 2019).

ETS-05 optimal light intensity corresponded to 100 $\mu\text{mol photons m}^{-2} \text{s}^{-1}$ reaching a dry weight of 1.13 g L^{-1} in 9 days. This was a promising result considering the 1.7 g L^{-1} obtained for *A. platensis* cultivated for 15 days in raceway ponds (Raeisossadati et al. 2019). It is also possible that, supplementing CO_2 , growth of ETS-05 could further increase. At lowest (25 $\mu\text{mol photons m}^{-2} \text{s}^{-1}$) and highest (400 $\mu\text{mol photons m}^{-2} \text{s}^{-1}$) intensities, biomass was reduced to a third or half. Direct correlation between EPS release and light intensity determined a higher EPS concentration at 400 $\mu\text{mol photons m}^{-2} \text{s}^{-1}$, indicating in this case the absence of a relationship between DW and EPS optima, as for *T. bouteillei* (Kvíderová et al. 2019). The positive effect of high light on EPS release was also observed in *Cyanobacterium aponinum* (Gris et al. 2017), *Nostoc* sp. (Ge et al. 2014a) and *Microcoleus vaginatus* (Ge et al. 2014b). Synthesis of phycobiliproteins behaved in the opposite way, with higher concentrations obtained at 25 $\mu\text{mol photons m}^{-2} \text{s}^{-1}$, decreasing up to 10 $\text{mg g}_{\text{DW}}^{-1}$ at 400 $\mu\text{mol photons m}^{-2} \text{s}^{-1}$. Chlorophyll *a* and total carotenoids content remained more or less similar in each intensity tested. There seems to be a trade-off between EPS and PC production, with optimal conditions for one being non advantageous for the other.

Interestingly, under low and high light, ETS-05 filaments had different lengths, while other morphological features

considered (cell dimension, shape, membrane thickness, internal arrangement) did not change. We hypothesized that high light exposure stimulates hormogonia formation in ETS-05. Their differentiation can be stimulated or inhibited by environmental factors, such as light and nutrients, in a species-specific manner (de Marsac 1994). As mentioned, hormogonia are involved in the release of exopolysaccharides called HPS (Risser and Meeks 2013), to enhance the gliding motility of these trichomes for dispersal. Part of the quantified EPS in higher light intensities could therefore be correlated with abundance of hormogonia.

Finally, nitrogen depletion was tested since it is known to enhance EPS release in *Nostoc* sp. BTA97, *Anabaena* sp. BTA990 (Tiwari et al. 2015) *Spirulina* sp. (Nicolaus et al. 1999) and *Cyanothece* sp. 113 (Su et al. 2007). However, no positive relation between the absence of this nutrient and EPS production in ETS-05. This condition was indeed too detrimental to the growth and synthesis of the compound of interest, even in a two-step cultivation system. Ultimately, it is important to notice the species-specific variability that characterizes EPS production in cyanobacteria, implying the requirement to verify the best condition for each strain.

Furthermore, from an industrial point of view, using the residual biomass of EPS and hydrophilic pigment extraction as starting material, carotenoids, and lipids (not evaluated in this study) could be obtained. In (Liu et al. 2016) was, for example, successfully verified an integrated production of triacylglycerols and astaxanthin (as a high-value carotenoid) using the microalgae *Chlorella zofingiensis*. Carotenoids from cyanobacteria can have various applications: anti-inflammatory, antioxidant, antitumor, color enhancer, anti-ageing agent for cosmetics (Pagels et al. 2021). Furthermore, chlorophylls present biotechnological applications as food colorant, for cosmetics production and for human health as anti-inflammatory, antioxidant and antitumor agents (da Silva Ferreira and Sant'Anna 2017).

Bioinformatic analysis of putative genes involved in EPS assembly and secretion was performed to hypothesize which mechanisms could be carried out in ETS-05. Results highlighted the presence in ETS-05 genome of Wzy-dependent, ABC transporter-dependent (Pereira et al. 2015) and HPS-linked pathways (Zuniga et al. 2020a). Moreover, other candidates were highlighted: proteins characterized by poly_export and SLBB domains, which can therefore act as OPX proteins. Real-Time qPCR allowed verification of the involvement of some of these putative genes: *wzc* (belonging to Wzy-dependent pathway), *ps_ex* (possibly coding for an OPX protein) and *hrmK* (probably involved in hormogonia formation), all augmented the expression when ETS-05 was exposed to optimal light, compared to low-light condition and the starting point.

To sum up, *wzc*, and *ps_ex* could be promising target genes to overexpress for an additional EPS assembly and release. On the other hand, enhancement of hormogonia

formation through *hrmK* could stimulate HPS release, but advantageous effects on biomass achievement should be further investigated.

Ultimately, the potential toxicity of *Phormidium* sp. ETS-05 was investigated, resulting in the absence of the genes involved in the synthesis of microcystin, cylindrospermopsin, saxitoxin, and lyngbyatoxin. These findings confirmed the absence of toxicity that was observed with an in vivo co-cultivation of ETS-05 and zebrafish (*Danio rerio*) larvae (Zampieri et al. 2020).

In this research *Phormidium* sp. ETS-05 was studied being the target species of the maturation process for the production of Euganean therapeutic muds, possessing for this reason an importance in the territory and in the obtainment of this unique product with verified bioactive properties. Moreover, these results showed that ETS-05 could represent an interesting organism for biotechnological applications, considering the limited resources needed for its cultivation and the numerous high value compounds produced. In particular, EPS synthesized by this species, which possess a demonstrated anti-inflammatory activity, can reach high yield when modulating the growth conditions. In addition to that, the absence of toxicity of the species is an important factor to consider in the optics of the use of its high value compounds for animal or human consumption and therapy. Finally, we investigated the transcription levels of several genes linked to EPS assembly and release by the organism with the hope of shed some light on this process that should gain more interest in the near future. The correlation between these genes' expression and the growth condition tested is a promising starting point for further characterizations and possible manipulations of ETS-05 to boost EPS productivity.

Supplementary Information The online version contains supplementary material available at <https://doi.org/10.1007/s10811-023-02995-0>.

Acknowledgements The authors wish to acknowledge Dr. Sara Zambolin for the enthusiastic contribution during her master thesis internship.

Authors' contributions Conceptualization: Nicoletta La Rocca, Raffaella Margherita Zampieri; Methodology: Nicoletta La Rocca, Raffaella Margherita Zampieri; Formal analysis and investigation: Raffaella Margherita Zampieri; Writing—original draft preparation: Raffaella Margherita Zampieri; Writing—review and editing: Nicoletta La Rocca, Fabrizio Caldara; Funding acquisition: Nicoletta La Rocca; Resources: Nicoletta La Rocca, Raffaella Margherita Zampieri; Supervision: Nicoletta La Rocca, Fabrizio Caldara.

Funding Open access funding provided by Università degli Studi di Padova within the CRUI-CARE Agreement. This work was supported by the Pietro d'Abano Thermal Studies Center (LA_R_EPPR18_01) and intramural grants by the Department of Biology of University of Padua.

Data availability The datasets generated during the current study are available from the corresponding author on reasonable request. *Phormidium* sp. ETS-05 genome is publicly available in NCBI under the BioProject PRJNA622676.

Declarations

Competing interests The authors have no competing interests to declare that are relevant to the content of this article.

Open Access This article is licensed under a Creative Commons Attribution 4.0 International License, which permits use, sharing, adaptation, distribution and reproduction in any medium or format, as long as you give appropriate credit to the original author(s) and the source, provide a link to the Creative Commons licence, and indicate if changes were made. The images or other third party material in this article are included in the article's Creative Commons licence, unless indicated otherwise in a credit line to the material. If material is not included in the article's Creative Commons licence and your intended use is not permitted by statutory regulation or exceeds the permitted use, you will need to obtain permission directly from the copyright holder. To view a copy of this licence, visit <http://creativecommons.org/licenses/by/4.0/>.

References

- Baer S, Heining M, Schwerna P, Buchholz R, Hübner H (2016) Optimization of spectral light quality for growth and product formation in different microalgae using a continuous photobioreactor. *Algal Res* 14:109–115
- Bennett A, Bogorad L (1973) Complementary chromatic adaptation in a filamentous blue-green alga. *J Cell Biol* 58:419–435
- Ceschi Berrini C, De Appolonia F, Dalla Valle L, Komárek J, Andreoli C (2004) Morphological and molecular characterization of a thermophilic cyanobacterium (Oscillatoriales) from the Euganean Thermal Springs (Padua, Italy). *Algol Stud/Arch Hydrobiol Suppl* 113:73–85
- Chamovitz D, Sandmann G, Hirschberg J (1993) Molecular and biochemical characterization of herbicide-resistant mutants of cyanobacteria reveals that phytoene desaturation is a rate-limiting step in carotenoid biosynthesis. *J Biol Chem* 268:17348–17353
- Cusick KD, Fitzgerald LA, Cockrell AL, Biffinger JC (2015) Selection and evaluation of reference genes for reverse transcription-quantitative PCR expression studies in a thermophilic bacterium grown under different culture conditions. *PLoS One* 10:0131015
- Da Silva Ferreira V, Sant'Anna C (2017) Impact of culture conditions on the chlorophyll content of microalgae for biotechnological applications. *World J Microbiol Biotechnol* 33:20
- de Marsac NT (1994) Differentiation of hormogonia and relationships with other biological processes. In: Bryant DA (ed) *The Molecular Biology of Cyanobacteria*. Springer, Berlin pp 825–842
- de Mooij T, de Vries G, Latsos C, Wijffels RH, Janssen M (2016) Impact of light color on photobioreactor productivity. *Algal Res* 15:32–42
- DuBois M, Gilles KA, Hamilton JK, Rebers PA, Smith F (1956) colorimetric method for determination of sugars and related substances. *Anal Chem* 28:350–356
- Ducat DC, Way JC, Silver PA (2011) Engineering cyanobacteria to generate high-value products. *Trends Biotechnol* 29:95–103
- Fioravanti A, Cantarini L, Guidelli GM, Galeazzi M (2011) Mechanisms of action of spa therapies in rheumatic diseases: What scientific evidence is there? *Rheumatol Int* 31:1–8
- Franks J, Stolz JF (2009) Flat laminated microbial mat communities. *Earth Sci Rev* 96:163–172
- Gan F, Zhang S, Rockwell NC, Martin SS, Lagarias JC, Bryant DA (2014) Extensive remodeling of a cyanobacterial photosynthetic apparatus in far-red light. *Science* 345:1312–1317
- Ge H, Xia L, Zhou X, Zhang D, Hu C (2014a) Effects of light intensity on components and topographical structures of extracellular polysaccharides from the cyanobacteria *Nostoc* sp. *J Microbiol* 52:179–183
- Ge H, Zhang J, Zhou X, Xia L, Hu C (2014b) Effects of light intensity on components and topographical structures of extracellular polymeric substances from *Microcoleus vaginatus* (Cyanophyceae). *Phycologia* 53:167–173
- Gris B, Sforza E, Morosinotto T, Bertucco A, La Rocca N (2017) Influence of light and temperature on growth and high-value molecules productivity from *Cyanobacterium aponinum*. *J Appl Phycol* 29:1781–1790
- Gris B, Treu L, Zampieri RM, Caldara F, Romualdi C, Campanaro S, La Rocca N (2020) Microbiota of the therapeutic euganean thermal muds with a focus on the main cyanobacteria species. *Microorganisms* 8:1590
- Han PP, Shen SG, Wang HY, Sun Y, Dai YJ, Jia SR (2015) Comparative metabolomic analysis of the effects of light quality on polysaccharide production of cyanobacterium *Nostoc flagelliforme*. *Algal Res* 9:143–150
- Herdman M, Rippka R (1988) Cellular differentiation: Hormogonia and baeocytes. *Meth Enzymol* 167:232–242
- Hirose Y, Chihong S, Watanabe M, Yonekawa C, Murata K, Ikeuchi M, Eki T (2019) Diverse chromatic acclimation processes regulating phycoerythrocyanin and rod-shaped phycobilisome in cyanobacteria. *Mol Plant* 12:715–725
- Kaplan D, Calvert HE, Peters GA (1986) The *Azolla-Anabaena azollae* relationship: XII. Nitrogenase activity and phycobiliproteins of the endophyte as a function of leaf age and cell type. *Plant Physiol* 80:884–90
- Khayatan B, Meeks JC, Risser DD (2015) Evidence that a modified type IV pilus-like system powers gliding motility and polysaccharide secretion in filamentous cyanobacteria. *Mol Microbiol* 98:1021–1036
- Kumar J, Singh D, Tyagi MB, Kumar A (2018) *Cyanobacteria: Applications in Biotechnology*. Elsevier, Amsterdam
- Kvídová J, Kumar D, Lukavský J, Kašťánek P, Adhikary SP (2019) Estimation of growth and exopolysaccharide production by two soil cyanobacteria, *Scytonema tolypothrichoides* and *Tolypothrix bouteillei* as determined by cultivation in irradiance and temperature crossed gradients. *Eng Life Sci* 19:184–195
- La Rocca N, Sciuto K, Meneghesso A, Moro I, Rascio N, Morosinotto T (2015) Photosynthesis in extreme environments: Responses to different light regimes in the Antarctic alga *Koliella antarctica*. *Physiol Plant* 153:654–667
- Laroche C (2022) Exopolysaccharides from microalgae and cyanobacteria: diversity of strains, production strategies, and applications. *Mar Drugs* 20:336
- Lima GM, Teixeira PCN, Teixeira CMLL, Filócomo D, Lage CLS (2018) Influence of spectral light quality on the pigment concentrations and biomass productivity of *Arthrospira platensis*. *Algal Res* 31:157–166
- Liu J, Mao X, Zhou W, Guarnieri MT (2016) Simultaneous production of triacylglycerol and high-value carotenoids by the astaxanthin-producing oleaginous green microalga *Chlorella zofingiensis*. *Bioresour Technol* 214:319–327
- Merel S, Walker D, Chicana R, Snyder S, Baurès E, Thomas O (2013) State of knowledge and concerns on cyanobacterial blooms and cyanotoxins. *Environ Int* 59:303–327
- Mistry J, Chuguransky S, Williams L, Qureshi M, Salazar GA, Sonhammer ELL, Tosatto SCE, Paladin L, Raj S, Richardson LJ, Finn RD, Bateman A (2021) Pfam: The protein families database in 2021. *Nucl Acids Res* 49:412–419
- Moran R (1982) Formulae for determination of chlorophyllous pigments extracted with N,N-dimethylformamide. *Plant Physiol* 69:1376–1381
- Nicolaus B, Panico A, Lama L, Romano I, Manca MC, De Giulio A, Gambacorta A (1999) Chemical composition and production of

- exopolysaccharides from representative members of heterocystous and non-heterocystous cyanobacteria. *Phytochemistry* 52:639–647
- Nwoba EG, Parlevliet DA, Laird DW, Alameh K, Moheimani NR (2019) Sustainable phycocyanin production from *Arthrospira platensis* using solar-control thin film coated photobioreactor. *Biochem Eng J* 141:232–238
- Ooms MD, Graham PJ, Nguyen B, Sargent EH, Sinton D (2017) Light dilution via wavelength management for efficient high-density photobioreactors. *Biotechnol Bioeng* 114:1160–1169
- Pagels F, Guedes AC, Amaro HM, Kijjoa A, Vasconcelos V (2019) Phycobiliproteins from cyanobacteria: Chemistry and biotechnological applications. *Biotechnol Adv* 37:422–443
- Pagels F, Vasconcelos V, Guedes AC (2021) Carotenoids from cyanobacteria: biotechnological potential and optimization strategies. *Biomolecules* 11(5):735
- Palinska KA, Deventer B, Hariri K, Łotocka M (2011) A taxonomic study on Phormidium-group (cyanobacteria) based on morphology, pigments, RAPD molecular markers and RFLP analysis of the 16S rRNA gene fragment. *Fottea* 11:41–55
- Patel A, Matsakas L, Rova U, Christakopoulos P (2019) A perspective on biotechnological applications of thermophilic microalgae and cyanobacteria. *Bioresour Technol* 278:424–434
- Paysan-Lafosse T, Blum M, Chuguransky S, Grego T, Pinto BL, Salazar GA et al (2022) InterPro in 2022. *Nucleic Acids Res* 51:D418–D427
- Pereira S, Zille A, Micheletti E, Moradas-ferreira P, de Philippis R, Tamagnini P (2009) Complexity of cyanobacterial exopolysaccharides: composition, structures, inducing factors and putative genes involved in their biosynthesis and assembly. *FEMS Microbiol Rev* 33:917–941
- Pereira SB, Mota R, Santos CL, De Philippis R, Tamagnini P (2013) Assembly and export of extracellular polymeric substances (EPS) in cyanobacteria. A phylogenomic approach. *Adv Bot Res* 65:235–279
- Pereira SB, Mota R, Vieira CP, Vieira J, Tamagnini P (2015) Phylum-wide analysis of genes/proteins related to the last steps of assembly and export of extracellular polymeric substances (EPS) in cyanobacteria. *Sci Rep* 5:14835
- Raesisosadati M, Moheimani NR, Parlevliet D (2019) Red and blue luminescent solar concentrators for increasing *Arthrospira platensis* biomass and phycocyanin productivity in outdoor raceway ponds. *Bioresour Technol* 291:121801
- Rippka R, Deruelles J, Waterbury JB (1979) Generic assignments, strain histories and properties of pure cultures of cyanobacteria. *J Gen Microbiol* 111:1–61
- Risser DD, Meeks JC (2013) Comparative transcriptomics with a motility-deficient mutant leads to identification of a novel polysaccharide secretion system in *Nostoc punctiforme*. *Mol Microbiol* 87:884–893
- Saini DK, Pabbi S, Shukla P (2018) Cyanobacterial pigments: Perspectives and biotechnological approaches. *Food Chem Toxicol* 120:616–624
- Sanfilippo JE, Garczarek L, Partensky F, Kehoe DM (2019) Chromatic acclimation in cyanobacteria: A diverse and widespread process for optimizing photosynthesis. *Annu Rev Microbiol* 73:407–433
- Schneider CA, Rasband WS, Eliceiri KW (2012) NIH Image to ImageJ: 25 years of image analysis. *Nat Meth* 9:671–675
- Singh S, Das S (2011) Screening, production, optimization and characterization of cyanobacterial polysaccharide. *World J Microbiol Biotechnol* 27:1971–1980
- Su C, Chi Z, Lu W (2007) Optimization of medium and cultivation conditions for enhanced exopolysaccharide yield by marine *Cyanosphaera* sp. 113. *Chin J Oceanol Limnol* 25:411–417
- Taboada B, Estrada K, Ciria R, Merino E (2018) Operon-mapper: A web server for precise operon identification in bacterial and archaeal genomes. *Bioinformatics* 34:4118–4120
- Tiwari ON, Khangembam R, Shamjetshabam M, Sharma AS, Oinam G, Brand JJ (2015) Characterization and optimization of biofloculant exopolysaccharide production by cyanobacteria *Nostoc* sp. BTA97 and *Anabaena* sp. BTA990 in culture conditions. *Appl Biochem Biotechnol* 176:1950–1963
- Toyoshima M, Toya Y, Shimizu H (2020) Flux balance analysis of cyanobacteria reveals selective use of photosynthetic electron transport components under different spectral light conditions. *Photosynth Res* 143:31–43
- Ward DM, Castenholz RW, Miller SR (2012) Cyanobacteria in geothermal habitats. In: Whitton BA (ed) *Ecology of cyanobacteria II: their diversity in space and time*. Springer, Dordrecht, pp 39–63
- Westermann M, Wehrmeyer W (1995) A new type of complementary chromatic adaptation exemplified by *Phormidium* sp. C86: Changes in the number of peripheral rods and in the stoichiometry of core complexes in phycobilisomes. *Arch Microbiol* 164:132–141
- Xie Y, Jin Y, Zeng X, Chen J, Lu Y, Jing K (2015) Fed-batch strategy for enhancing cell growth and C-phycocyanin production of *Arthrospira* (*Spirulina*) *platensis* under phototrophic cultivation. *Bioresour Technol* 180:281–287
- Zampieri RM, Adessi A, Caldara F, Codato A, Furlan M, Rampazzo C, De Philippis R, La Rocca N, Dalla Valle L (2020) Anti-inflammatory activity of exopolysaccharides from *Phormidium* sp. ETS05, the most abundant cyanobacterium of the therapeutic euganean thermal muds, using the zebrafish model. *Biomolecules* 10:582
- Zampieri RM, Adessi A, Caldara F, De Philippis R, Dalla Valle L, La Rocca N (2022) In vivo anti-inflammatory and antioxidant effects of microbial polysaccharides extracted from Euganean therapeutic muds. *Int J Biol Macromol* 209:1710–1719
- Zuniga EG, Boateng KKA, Bui NU, Kurnfuli S, Muthana SM, Risser DD (2020a) Identification of a hormogonium polysaccharide-specific gene set conserved in filamentous cyanobacteria. *Mol Microbiol* 114:597–608
- Zuniga EG, Figueroa NM, Gonzalez A, Pantoja AP, Risser DD (2020b) The hybrid histidine kinase HrmK is an early-acting factor in the hormogonium gene regulatory network. *J Bacteriol* 202:e00675-e719

Publisher's note Springer Nature remains neutral with regard to jurisdictional claims in published maps and institutional affiliations.